Measurement of Three-Dimensional Permeability

J.R. Weitzenböck, R.A. Shenoi*, P.A. Wilson
Department of Ship Science, University of Southampton,
Highfield, Southampton, SO17 1BJ, United Kingdom
(*to whom correspondence should be addressed)

Abstract

The paper investigates the possibility of using a three-dimensional radial flow test to measure permeability. As part of this investigation, compaction tests have been conducted to determine the fibre volume fraction as a function of the compaction pressure. The effect of the closing speed has been investigated. Results from permeability tests are reported. The flow front in these tests is measured using thermistors. An important facet of the results is the dependence of the flow front progression on capillary pressure. Finally new possible applications for the flow measurement sensor are discussed.

1. Introduction

The traditional moulding techniques to produce fibre reinforced plastic (FRP) boats and small ships are by hand lay-up and spray-up. However economic pressure and increasingly stringent environmental requirements on styrene emission make these techniques less acceptable. One of the possible alternatives is injection moulding. This includes Resin Transfer Moulding (RTM) and vacuum assisted RTM, both of which are receiving increasing attention from manufacturers of large FRP structures in many fields. While RTM is a well established moulding process for small and thin components there are still a number of practical problems when utilising RTM to mould thick components. One issue is the reliable and economical measurement of three-dimensional permeability.

The most common method to measure permeability in the out-of-plane direction is to use the one-dimensional channel flow apparatus (transplane measurement device) with constant flow rate (Trevino 1991, Wu 1993 and 1994). To calculate the through-thickness permeability, Darcy's law for one dimensional flow is used. The in-plane permeabilities are determined from two-dimensional flow experiments. Trevino et al. 1991 found that most reinforcement materials showed a dependence of through the thickness permeability on stack thickness. This is probably due to the fact that only a very small stack thickness was used (permeability values were given for a thickness of 3.2mm!). In addition to the transplane permeability tests, Wu et al. 1993 and 1994 performed a three-dimensional radial flow experiment with a circular preform (thickness 18mm). Since the in-plane permeability of that particular material was known from two-dimensional tests, a flow simulation program was employed to match the inlet pressure by selecting an appropriate value for the through-thickness permeability. It was found that the permeability values obtained from the transplane measurement device were about 10 to 15% larger than the simulated permeability values. This was attributed to edge leaking effects in the transplane measurement device.

Woerdeman et al. 1995 have proposed the use of the one-dimensional channel flow technique to determine the six components of the three-dimensional permeability tensor. For six different directions, the effective permeability was derived as a function of the rotation angles and the principal permeabilities which is then solved numerically for the principal permeabilities. However the complex algebra conceals the fact that the suggested experiments are not sufficient to determine the full

permeability tensor. The simplest way to show this is by inspecting the tensor components. There are three components (K_{xz}, K_{yz}, K_{zz}) which contain out-of-plane information. These cannot be determined independently with two out-of-plane tests as proposed. Hence three (instead of four) in-plane and three out-of-plane experiments (of which two are not aligned with the z-axis) are required to determine the full three-dimensional tensor. These out-of-plane experiments are very difficult to perform. Hence the practical value of this method is limited.

The approach suggested by Ahn et al. 1995 is the first attempt to use a single three-dimensional flow experiment to measure the three-dimensional permeability tensor. Fibre optics permit the measurement of the flow front within the cavity. This paper is an attempt to compare different measurement techniques, namely the pressure drop (channel flow), flow visualisation (two-dimensional radial flow) and fibre optics (three-dimensional radial flow) technique. The three-dimensional radial flow technique differs from the through-thickness permeability measurement techniques discussed so far, as it measures the progression of the flow front rather than the flow rate. This type of flow is called unsaturated flow. However only thin moulds were used (6.4 to 9.5mm) for the three-dimensional radial flow experiment. Furthermore because of the mould material used (Plexiglas) considerable deflection would be expected at higher fibre volume fractions. The way, in which the data has been analysed is questionable. Six permeability values were obtained from three-dimensional radial flow experiments. But only a single (!) value was used in the further analysis from which it was concluded that the three measurement techniques agreed well.

Wu et al. 1993 and 1994 also investigated the influence of clamping pressure on permeability. It was found that as soon as the inlet pressure exceeds the clamping pressure, the relation between pressure and flow rate becomes non-linear (a violation of Darcy's law). This effect was explained by additional compaction caused by the high flow rates. As long as the injection pressure was less than the clamping pressure this effect was not observed. Hence an understanding of the compaction behaviour is essential for successful permeability measurement.

Toll and Månson 1994 derived a power law from micromechanical analysis which describes the compaction of woven fabrics and random mats well. Pearce and Summerscales 1995 investigated the time dependence of the compaction pressure for a plain weave fabric. It was shown that once the target peak load was reached and the crosshead of the testing machine was stopped the load started to relax. It was then possible to reduce the gap height further. Pearce and Summerscales found that it was possible to describe this relaxation with an exponential equation. It was demonstrated that a single layer yields a higher fibre volume fraction for the given pressure while three, four or five layers yield (almost) identical results.

The aims of this paper are two-fold: (a) to discuss results from compaction experiments and its significance to permeability measurement; (b) to highlight the limits of three-dimensional radial flow permeability experiments.

2. Experiments

2.1 Aim of experiments

The purpose of the compression tests has been to measure the required compaction pressures for fabrics and to find the permissible fibre volume fractions for various compaction pressures. At the same time the time-dependence of the compaction pressure was investigated to ensure that the flow experiment would be carried out at the desired compaction pressure (to avoid fluid-induced compaction). The aim of the permeability experiments has been to explore the limits of the flow measurement technique and theory for permeability calculation.

2.2 Compaction tests

The fibre volume fraction is calculated according to Pearce and Summerscales (1995)

$$V_f = \frac{N W_f}{d \rho} \qquad (2.1)$$

where V_f is the fibre volume fraction, N is the number of layers, W_f is the weight per unit area of the fabric, d is the height of the cavity and is ρ the density of the fibres. Materials tested were a continuous filament mat (Unifilo U750-450), a woven roving (RT600), a twill fabric (RC600) all from Vetrotex and a quasi-unidirectional non crimp fabric from Tech Textiles (E-LPb 567). The tests were done in a universal testing machine (JJ Instruments; 30 kN load cell) which was fitted with a compression jig. The size of the platens was 55 mm by 78 mm. All tests were carried out with four layers of fabric. The crosshead speed and the lay-up sequence for each experiment are shown in Table 1. "0" means the unidirectional fibres are aligned with the longer side of the platens while "90" denotes that the fibres are aligned at 90 degrees to this direction. To calculate the weight per unit area the side lengths of the samples were measured with a vernier calliper while the weight of the samples was measured using a top pan balance.

2.3 Permeability measurement

Data analysis

Permeability is calculated from the flow front position measured at various time steps. To detect the flow front, thermistors are placed at different locations through the depth and width of the mould lay-up (Figure 1). The theory to calculate the permeability from the experimental flow front measurements has been presented in Weitzenböck et al. (1995a). It assumes that the measurement coordinate system is aligned with the principal coordinate axes. The expressions for the three principal permeabilities are repeated below.

$$K_1 = \frac{\mu\varepsilon}{6\Delta P}\left[\frac{2x_f^3}{x_o} - 3x_f^2 + x_o^2\right]\frac{1}{t} \qquad (2.2)$$

$$K_2 = \frac{\mu\varepsilon}{6\Delta P}\left[\frac{2y_f^3}{y_o} - 3y_f^2 + y_o^2\right]\frac{1}{t} \qquad (2.3)$$

$$K_3 = \frac{\mu\varepsilon}{6\Delta P}\left[\frac{2z_f^3}{z_o} - 3z_f^2 + z_o^2\right]\frac{1}{t} \qquad (2.4)$$

where μ is the fluid viscosity, ε is the porosity, ΔP is the pressure gradient between inlet and flow front, x_f, y_f and z_f are the flow front radii measured along the x,y and z-axis respectively, x_o, y_o and z_o are the inlet diameter in the x, y and z direction and t is the time. Ahn et al. 1995 have independently derived equations identical to (2.2), (2.3) and (2.4). In practice considerable difficulty arises from the fact that z_o is required to evaluate equation (2.4). It is extremely difficult to measure z_o directly from experiments. While x_o and y_o are equal to the inlet radius it was assumed that z_o is one tenth of the inlet radius.

To validate the in-plane permeability obtained from the three dimensional tests a series of two-dimensional flow tests was conducted. The data analysis algorithm used here differs from the algorithm published in Weitzenböck et al. (1995a) as it enables the calculation of the principal permeability regardless of the measurement direction. Details can be found in Weitzenböck (1996).

Experimental set-up

The experimental rig used for the permeability measurement has an aluminium work surface with a glass top plate of 400 x 400 x 25 mm. A PC is utilised to record and process inlet pressure transducer and thermistor readings. To measure the in-plane flow front position six thermistors, see Figure 2 for schematic (Weitzenböck et al. (1995b)), are linked together with thin (less than 1mm wide) strips of masking tape. Figure 3 shows a schematic of the multiple flow sensor. In addition fibre bundles are twisted around every wire but the last one to stop unwanted channelling along the wires. This helped to simplify the lay-up process considerably. The x,y coordinates of each thermistor head are measured using a tape measure while the through-thickness coordinate is calculated from the ratio of the layer on which the thermistor has been placed to the total number of layers in the stack. This assumes a homogeneous compaction of the fibre mats. All the tests were radial flow tests with constant pressure injection either at 100kPa or 200kPa. The test fluid was Shell Vitrea M100 oil with a viscosity of 330 mPa at 18^{0}C. The twill fabric tested was the RC 600 from Vetrotex. The thickness of the cavity was 4.65mm for the two-dimensional test and 20mm for the three-dimensional flow tests. To ensure a uniform inlet condition for the two-dimensional tests a 12.7mm diameter hole was punched at the centre of each layer. The diameter of the inlet is 10.5mm. For the two-dimensional tests 10 and 12 layers were used - for the three-dimensional tests there were 44 layers.

3. Discussion of results

3.1 Compaction tests

Weight per unit area

The results of this investigation are summarised in Table 2. It shows that for all materials a difference to the nominal weight can be observed. During this investigation it was found that for the woven fabrics, in particular twill fabric, it was very difficult to obtain an accurate measure of the size and weight since these fabrics tend to fray very easily even if handled carefully. All samples are taken from the first metre of each roll.

In the case of the random mat and the twill fabric, the number of samples is very small. Furthermore the deviation from the nominal weight is small too. Hence it was decided to use the nominal weight for random matt (450 g/m^2) and twill fabric (600 g/m^2) to determine the fibre volume fraction. The weight of the woven roving is based on a larger population. Also the standard deviation is quite small which increases the confidence in the measured value. Therefore 588 g/m^2 was used for woven roving for the subsequent calculations. Most surprising was the weight for the unidirectional material of 660 g/m^2 which is a significant deviation from the 567 g/m^2 as quoted by the manufacturer. However consulting Tech Textiles revealed that the quoted weight only applies to the unidirectional tows. The weight for the weft (60-80 g/m^2) and the powder coating has to be added to the nominal weight.

Compaction behaviour

For all experiments the samples were compacted at the given crosshead speed until the target pressure of 200kPa was reached. The crosshead was then stopped and a relaxation of the load was observed. After about 8 minutes the crosshead was moved again to reach the target pressure. The second compaction changed the thickness of the sample very little. Therefore only the initial compaction is reported for the following experiments. A typical result is shown in Figure 4. For the woven and non-crimp fabric the initial relaxation after 8 min was about 10% while after the second compaction a relaxation of 5-7% was noted. For the random mat it was 25 and 15% respectively. For the purpose of designing the permeability experiments 1% was added to the fibre volume fraction value (which was measured after the initial compaction) to compensate for the relaxation.

Important for the planning of injection experiments is the variation of the compaction pressure with fibre volume fraction which is shown for unidirectional (UD) and woven roving (WR) in Figure 5. It was interesting to note that the unidirectional fabric in the 0/90 lay-up showed a slightly higher fibre volume fraction than the 0/0 lay-up. This could be observed for single and mixed lay-ups (UD and WR, WR/UD/WR/UD). The same effect was not observed for the WR/WR/UD/UD lay-up sequence which yielded slightly lower fibre volume fractions for a given pressure. It was observed that the fibre volume fraction of the mixed lay-ups was higher than the fibre volume fractions of the individual fabrics (WR and UD with 0/0 and 0/90 orientation). This is in agreement with trends observed by Batch and Cumiskey (1990). The fibre volume fraction of the mixed lay-up was calculated from equation (2.1) using the average weight per unit area of the two fabrics.

Figure 6 shows compaction pressure versus fibre volume fraction for unidirectional and twill fabric (T). As before the combination of single layers of each fabric (T/UD/T/UD) yielded a higher fibre volume fraction than the T/T/UD/UD lay-up sequence. However in comparison with the woven roving results the values obtained here are slightly smaller (about 1% V_f). The fibre volume fraction for four layers of twill fabric had to be estimated since the final compaction thickness was too low (perhaps as a result of a reading error). The thickness of 1 mm compared with 1.6 to 1.7 mm for all the other experiments would have yielded a fibre volume fraction of about 90%. It was found that the compression jig was not ideal for testing the twill fabric. Because of its design the specimens had to be cut to size which allowed only very little overhang to make up for the frayed edges.

In addition to the above investigation the effect of various closing speeds of the crosshead on the compaction behaviour was examined, see Figure 7. The results indicate that although the speed was increased by a factor of 20 (0.1 mm/min, 0.5 mm/min and 2 mm/min) the effect on the pressure versus fibre volume fraction curve was minimal. It has to be noted however that even though 2mm/min is higher than closing speeds used in other investigations on compaction behaviour, it is still very slow compared with stamping processes used for mass preform fabrication.

3.2 Three-dimensional permeability

Results

The results of the permeability tests are shown in Table 3. Runs 1 to 4 are two-dimensional flow experiments with a gap height of 4.65mm which are used for control purposes. Runs 5 and 7 are the results from tests with 20mm gap height and 44 layers of twill fabric. Run 5 compares well with the two-dimensional results. This is not the case for run 7 which is at least one order of magnitude larger than the other results.

It was observed in most experiments that the flow front was quite irregular, in particular for small radii. In many cases the flow front was hexagonal which later became elliptical (it followed the diagonal of the crossover points of the twill fabric). In one case (run 3) the flow front was almost circular! Also, for large flow front radii, the flow front sometimes developed a "sharp tooth" at various points along the flow front (run 2 and 4).

For run 5 it was observed that the flow front velocity was very slow - it took three hours to complete the experiment. There seemed to be no sharp flow front any more further away from the inlet. This could be seen when the flow front reached the glass plate. Initially only the fibre bundles were wetted with oil - the pores were filled later (after four to five minutes). As a consequence the thermistor readings do not give a very distinct reading any more. The voltage changes very slowly with a total voltage drop of the same order as for faster fluid velocities. The other three-dimensional flow test (run 7) showed a completely different behaviour. The test was completed in less than 8 minutes. After about one minute oil was emerging from one side. It appeared that the oil had formed a channel between the base plate of the mould and the fibres hence accelerating the flow. The wet out in the vertical direction was then

taking place over virtually the whole area of the sample hence the remarkable difference in the fill time (and permeability).

In general it was observed that the flow front in the part of the mould where the thermistor sensors had been placed was lagging behind compared with other undisturbed parts of the mould. Furthermore when oil started to emerge from the side of the mould in run 7 it first appeared in a region with no thermistors. The reason for that is probably local compaction due to the presence of the thermistors. The efforts to try to reduce the channelling along the thermistor wires increases the thickness of the whole sensor which invariably reduces the fibre volume fraction. It appears that the balance between these two opposing factors has yet to be found. For future tests it seems advisable to use smaller fibre bundles and to increase the thermistor spacing.

Thermistor signal

By analysing the variation of the thermistor voltage as a function of time, it is possible to extract more information than the time the flow front takes to reach the thermistor position. Figure 8 shows voltage readings of four thermistors positioned along the x-axis (run 5). It is interesting to observe how the thermistor response changes with time (and increasing distance away from the inlet). First there is a very sharp drop (thermistor 3) which slowly starts to become more rounded (6 and 9). In addition a second hump is forming in the lower part of the voltage drop curve (black arrow, 9 and 12). A possible explanation could be that initially there is only macroscopic flow in the pores resulting in the sharp drop of thermistor 3. Capillary flow develops as well, but this is still part of the macroscopic flow front (6). As time progresses, capillary flow is leading the macroscopic flow front by several minutes (observed in run 5) so that the initial curve is caused by capillary flow while the second hump marks the arrival of macroscopic flow front (thermistors 9 and 12).

It is possible to combine point-wise measurements of flow front to obtain an estimate of the orientation of the flow front. Figure 9 shows the lay-up which was used in run 7. The flow front first reached thermistor 28 (t = 31.31s), then thermistor 31 (t = 36.80s) and finally thermistor 34 (t = 39.55s). The result for the third thermistor is probably not very accurate as it lies in the wake of the thermistors 28 and 31. The flow times for the first two thermistors indicate that the flow front has more advanced in the y-direction than in the x-direction. This agrees well with the flow patterns which were observed in the experiment. Oil was emerging at the left hand side (negative x-direction) first and last on the right hand side (positive x-direction) where most of the thermistors were placed. This is another indication that a series of thermistors does increase the fibre volume fraction.

It was also observed that there is some correlation between the fluid velocity and the voltage reading of the thermistor in the wetted domain. Figure 10 shows the voltage versus time plot for a thermistor close to the inlet. It clearly shows that the voltage increases with time indicating a drop in velocity (in accordance with the theory). More work is required to correlate voltage measurements with fluid velocity.

Figure 11 shows the voltage readings of the thermistors which were placed directly above the inlet (run 7). Soon after the start of the injection (~1.5 seconds) a drop in the voltage of all thermistors can be observed. This is clear evidence that with the start of injection the fabric was compacted further, resulting in a channel forming between the fibres and the bottom of the mould. Comparing the thermistor voltage readings for runs 1 to 4 reveal similar voltage drops between the two fibre volume fractions used.

Capillary effects

One way to explain the observed flow patterns is by comparing the pressure distribution of three-dimensional spherical flow with one-dimensional channel flow and two-dimensional radial flow. The

pressure distributions are given by the following equations (assuming atmospheric pressure at the flow front):

$$P(x)_{channel} = P_o \frac{x_f - x}{x_f - x_o} \qquad (3.1)$$

$$P(x)_{radial} = P_o \frac{\ln(x/x_f)}{\ln(x_o/x_f)} \qquad (3.2)$$

$$P(x)_{spherical} = P_o \frac{x_f\, x_o}{x_f - x_o}\left(\frac{1}{x} - \frac{1}{x_f}\right) \qquad (3.3)$$

where P_o is the inlet pressure, x_o is the inlet radius and x_f is the flow front length. In Figure 12 the pressure distributions are compared for a given flow front length. This reveals great differences both in magnitude and gradient of the spherical flow compared with the other two tests. This observation is confirmed by plotting the pressure gradient at the flow front for various flow front lengths (Figure 13). The small pressure gradient and the low absolute pressure value at the flow front for the spherical flow case suggest strongly that capillary pressure could be more important than the externally applied inlet pressure.

Analysis of the flow pattern can be performed using the cross-over length L_{cv}, which is a measure of the importance of capillary pressure. This concept was introduced by Wong (1994). First the ratio of the applied pressure and capillary pressure is determined; this entity, Ca_{mod}, is termed the modified capillary number.

$$Ca_{mod} = \frac{\Delta P}{P_c} \qquad (3.4)$$

ΔP is defined as the pressure drop across a pore or fibre with diameter D_f. and P_c is the capillary pressure. Wong (1994) then defines the cross-over length as follows:

$$L_{cv} = \frac{D_f}{Ca_{mod}} \qquad (3.5)$$

In order to minimise the capillary effects one has to ensure that the fabric samples used in the flow experiments are larger than L_{cv} . Equation (3.5) has been derived for one-dimensional flow with constant flow rate. In this case the pressure gradient is constant through-out the experiment. However this is not true for constant inlet pressure experiments where L_{cv} becomes a function of the flow front radius.

The capillary pressure P_c can be defined for a fibrous preform as (Ahn et. al. (1991)):

$$P_c = \frac{F}{D_e}\gamma \cos\theta \qquad (3.6)$$

and

$$D_e = D_f \frac{\varepsilon}{(1-\varepsilon)} \qquad (3.7)$$

where γ is the surface tension of the fluid, θ is the contact angle between fluid and fibre, F is the form factor which depends on fibre alignment and the flow direction, D_e is the equivalent pore diameter and ε is the porosity. For flow along a bundle of fibres $F = 4$, while, for flow across a fibre bundle $F = 2$. For flow in the through-thickness direction Ahn et. al. (1991) determined experimentally $F = 1.8$ for a plain weave fabric. In three-dimensional flow all these flow situations are present. Hence $F = 3$ is assumed for the following calculations. Capillary flow occurs at the flow front hence pressure needs to be evaluated at $x = x_f - D_e$ to obtain Ca_{mod}. This is done using equations (3.1) to (3.3). Note that to reflect the

fibrous structure of the material D_e is used instead of D_f to calculate ΔP and L_{cv}. The following values have been used: P_o =100kPa, ε = 0.484, D_f = 3.36x10^{-5} m (Carleton and Nelson (1994)), γ = 0.0322 N/m (oil, Steenkamer et. al. (1995)) and θ = 0° (oil, Steenkamer et. al. (1995)).

The cross-over lengths for the one, two and three-dimensional flow have been compared in Figure 14. It can be seen from this figure that L_{cv} for spherical flow is about one order of magnitude larger than L_{cv} for both the radial and channel flow. A plot of the ratio of L_{cv} versus flow front illustrates these observations better (Figure 15). It shows that L_{cv} for spherical flow very quickly becomes the same order of magnitude as the flow front, making reliable tests impossible as observed in the experiments. To reduce L_{cv} one has to increase Ca_{mod} either by increasing the inlet pressure or by increasing the radius of the inlet. However increasing the inlet pressure will increase the risk of flow induced compaction rendering any measurement results useless for permeability calculation. Increasing the inlet radius will make the diameter of the inlet larger than the thickness of the mould. The interpretation of the results will be more difficult as the analytical formulae used here, equations (3.1) to (3.3), assume a hemispherical inlet which is violated in the experiment.

Comparison with literature

The importance of capillary pressure as observed here seems to be in contrast with the results reported in Weitzenböck et al. (1995b) where the three-dimensional radial flow technique was used successfully to measure permeability of continuous filament random mat (Vetrotex U750-450). This can be explained by the difference in the structure of the random mat and the twill fabric used in this paper. The twill fabric consists of tightly woven bundles of fibres while in the case of random mat thin strands of fibres are laid up in circular loops. As a consequence the effective pore diameter of the random mat is considerably larger than the effective pore diameter for the twill fabric. More importantly this leads to a reduction of the capillary pressure and at the same time increases ΔP . These two effects reduce L_{cv}. Hence it is possible to measure permeability of random mat with the three-dimensional radial flow technique tough not that of twill fabric.

The results presented in this section do tie in with observations made by other researchers. Ahn et al. (1995) only uses a 9.5mm thick mould. Over this distance the thermistors gave useful results. At the same time as Figure 12 has shown small disturbances will have a profound effect on the pressure distribution and hence permeability results. This will tend to make the test not very reliable and repeatable. Similar observations were made by Trevino et al. (1991). They found that for the one-dimensional channel flow test, a dependence of the through-thickness permeability on the stack thickness if the thickness was small. In later publications (Wu et al. 1994) a three-dimensional radial flow experiment was introduced where the through-thickness permeability was calculated numericaly. For reliable permeability measurement a stack thickness of at least 15mm was specified. As this was a steady state flow experiment with saturated flow, no problems with capillary pressure were encountered. It has to be noted however that in this experiment the outside boundary of the fabric samples is also the boundary of the flow domain. Therefore dimensional accuracy is most important. This is very difficult to achieve for circular fabric samples, which are required for this experiment.

4. Conclusions

In this paper the possibility of using a three-dimensional radial flow test to determine the full permeability tensor in a single experiment has been investigated. It was found that for accurate permeability measurement it is necessary to measure the weight of the fabric. It was also observed that permeability was influenced by flow induced compaction. For three-dimensional permeability tests with unsaturated flow it was noticed that capillary flow was the dominant flow pattern. The only way to overcome this is by increasing the inlet pressure. However this led to flow-induced compaction and easy flow paths that rendered any results useless. These problems were not encountered for flow tests with random mat. However, most thick laminates are used in structural applications where woven and non-

crimp fabrics are employed as reinforcement material. Therefore it has to be concluded that three-dimensional radial flow tests with unsaturated flows are not suitable for permeability measurement. The only option to obtain out-of-plane permeability data is to use one- and possibly three-dimensional steady state flow tests with saturated flow.

The use of thermistors for permeability measurement purposes is questionable as the reduction in local channelling along the wires leads to an increase in fibre volume fraction. However it was demonstrated that a smaller number of thermistors is an ideal tool for process control and validation of flow simulations as they yield information about the impregnation process, the orientation of the flow front, compaction of the fibres and possibly the fluid velocity.

Acknowledgements

The authors would like to thank Vetrotex (UK) Ltd for the donation of raw materials.

References

AHN, K. J., Seferis, J. C. and Berg, J. C., (1991), Simultaneous Measurements of Permeability and Capillary Pressure of Thermosetting Matrices in Woven Fabric Reinforcements, *Polymer Composites*, June, Vol. 12, No. 3, p. 146-152

AHN, S. H., Lee, W. I. and Springer, G. S., (1995), Measurement of the Three-Dimensional Permeability of Fiber Preforms Using Embedded Fiber Optic Sensors, *Journal of Composite Materials*, Vol. 29, No. 6, p. 714-733

BATCH, G. L. and Cumiskey, S., (1990), Multilayer Compaction and Flow in Composites Processing, *45th Annual Conference*, Reinforced Plastics/ Composites Institute, The Society of the Plastics Industry Inc., Washington D.C., February 12-15, session 9 - A, 11 pages

CARLETON, P. S. and Nelson, G. S., (1994), Wetout of Glass Fiber Tows in Structural Reaction Molding I. Capillary Action and Fiber Mobility, *Journal of Reinforced Plastics and Composites*, Vol. 13, January, p. 20-37

PEARCE, N. and Summerscales, J., (1995), The Compressibility of a Reinforcement Fabric, *Composites Manufacturing*, Vol. 6, No. 1, p. 15-21

TOLL, S. and Månson, J.-A. E., (1994), An Analysis of the Compressibility of Fibre Assemblies, *6th International Conference on Fibre Reinforced Composites (FRC'94)*, University of Newcastle upon Tyne, U. K., 29-31 March, Paper 25, 10 pages

TREVINO, L., Rupel, K., Young, W. B., Liou, M. J. and James Lee, L., (1991), Analysis of Resin Injection Molding in Molds With Preplaced Fiber Mats. I: Permeability and Compressibility Measurements, *Polymer Composites*, Vol. 12, No. 1, p. 20-29

STEENKAMER, D. A., McKnight, S. H., Wilkins, D. J. and Karbhari, V. M., (1995), Experimental characterization of permeability and fibre wetting of liquid moulding, *Journal of Material Science*, Vol. 30, p. 3207-3215

WEITZENBÖCK, J. R., Shenoi, R. A. and Wilson, P. A., (1995a), Characterization of Resin Flow Through Thick Laminates in Resin Transfer Moulding, *10th International Conference on Composite Materials (ICCM/10)*, Whistler, Canada, 14-18 August, Vol. III, p. 301-308

WEITZENBÖCK, J. R., Shenoi, R. A. and Wilson, P. A., (1995b), Flow Front Measurement in RTM, *4th International Conference on Automated Composites (ICAC '95)*, Nottingham, 6-7 September, Vol. 2, p. 307-314

WEITZENBÖCK, J. R., (1996), *Flow Characterization in Resin Transfer Moulding*, Ph.D. thesis, University of Southampton, in preparation

WOERDEMAN, D. L., Phelan, F. R. and Parnas, R. S., (1995), Interpretation of 3-D Permeability Measurements for RTM Modeling, *Polymer Composites*, Vol. 16, No. 6, p. 470-480

WONG, P.Z., (1994), Flow in Porous Media: Permeability and Displacement Patterns, *MRS Bulletin*, May, p. 32-38

WU, C. H., Wang, T. J. and Lee, L. J., (1993), Permeability Measurement and its Application in Liquid Composite Molding, *48th Annual Conference*, Composites Institute, The Society of the Platics Industry Inc., 8-11 February, Session 8-E, 10 pages

WU, C. H., Wang, T. J. and Lee, L. J., (1994), Trans-Plane Fluid Permeability Measurement and Its Applications in Liquid Composite Molding, *Polymer Composites*, Vol. 15, No. 4, p. 289-298

Tables and figures

Run No.	Type of fabric	Lay-up sequence (orientation)	Crosshead speed
2	U750-450	-	0.5 mm/min
4	Woven Roving	-	0.1 mm/min
6	UD	0/0	0.1 mm/min
8		0/90	0.1 mm/min
10	WR/UD	WR/UD/WR/UD (0/0)	0.1 mm/min
12		WR/UD/WR/UD (0/90)	0.1 mm/min
14		WR/WR/UD/UD (0/0)	0.1 mm/min
16		WR/WR/UD/UD (0/90)	0.1 mm/min
A		WR/UD/WR/UD (0/0)	0.1 mm/min
B		WR/UD/WR/UD (0/0)	0.5 mm/min
C		WR/UD/WR/UD (0/0)	2.0 mm/min
D	Twill/UD	Twill/UD/Twill/UD (0/0)	0.1 mm/min
E		Twill/Twill/UD/UD (0/0)	0.1 mm/min
F	Twill	-	0.1 mm/min

Table 1 Details of compaction experiments

	U750	Woven Roving	UD	Twill
nominal weight	450	600	567	600
mean	458.77	588.47	660.80	616.05
standard deviation	26.97	15.43	9.98	36.09
number of samples	4	18	26	8

Table 2 Weight per unit area [g/m^2]

Run no	K_1	K_2	K_3	V_f [%]	P_o [Pa]
1	5.66×10^{-11}	2.43×10^{-11}	-	50.4	$1.10 \times 10^{+5}$
2	2.36×10^{-11}	1.32×10^{-11}	-	60.5	$1.06 \times 10^{+5}$
3	4.74×10^{-11}	4.39×10^{-11}	-	50.4	$2.00 \times 10^{+5}$
4	2.68×10^{-11}	1.06×10^{-11}	-	60.5	$1.95 \times 10^{+5}$
5	2.98×10^{-11}	1.80×10^{-11}	1.08×10^{-12}	51.6	$1.01 \times 10^{+5}$
7	3.75×10^{-9}	1.16×10^{-9}	1.06×10^{-11}	51.6	$1.85 \times 10^{+5}$

Table 3 Results from permeability tests

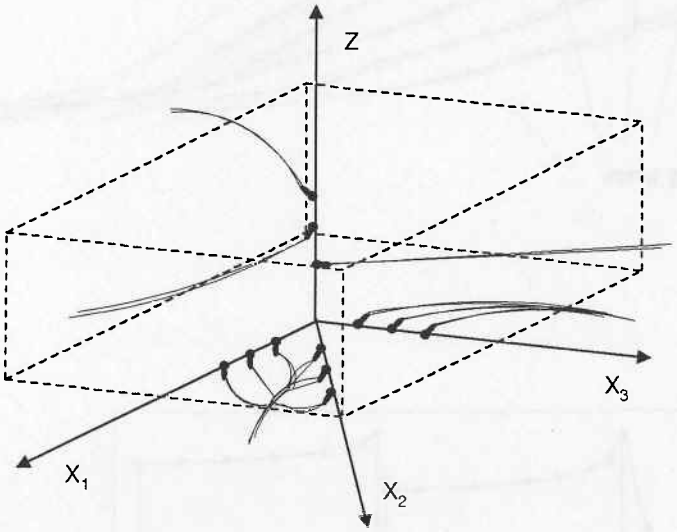

Figure 1 Lay-up of thermistors in mould

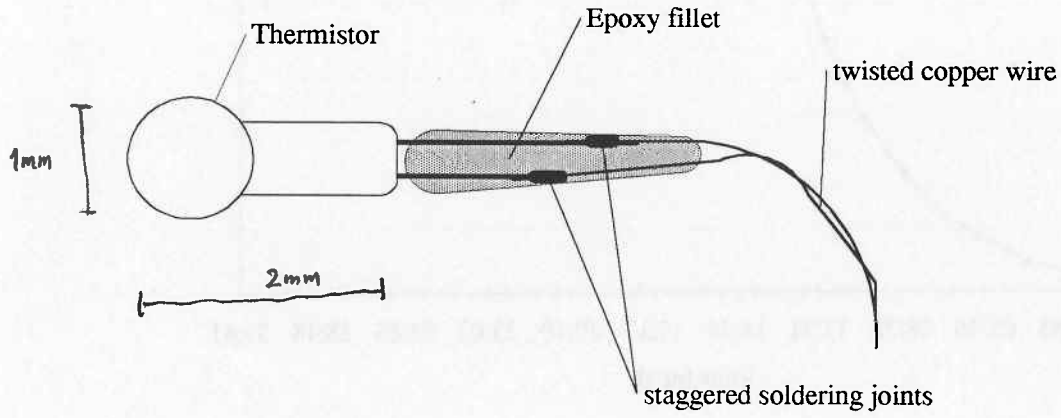

Figure 2 Thermistor sensor

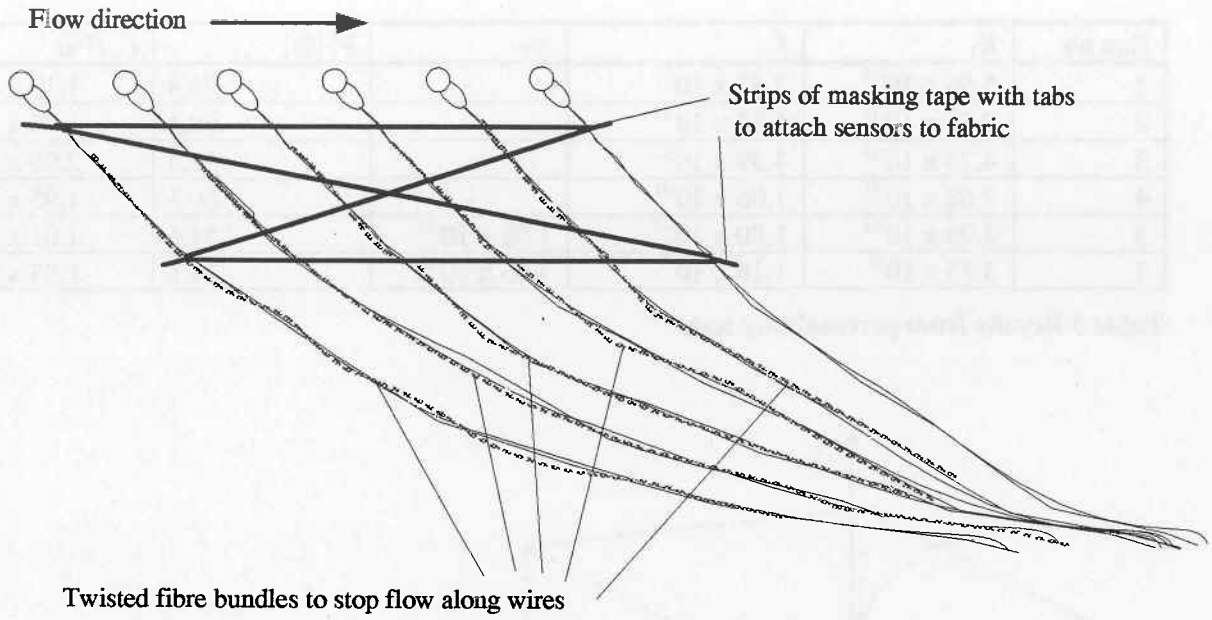

Figure 3 Multiple flow sensor

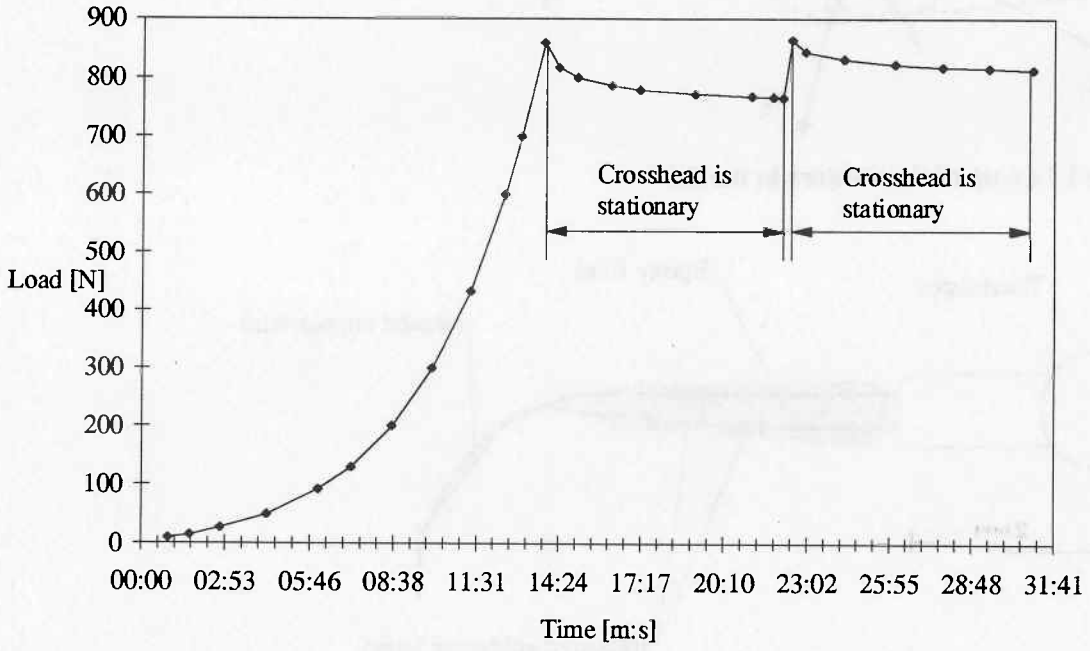

Figure 4 Load versus time

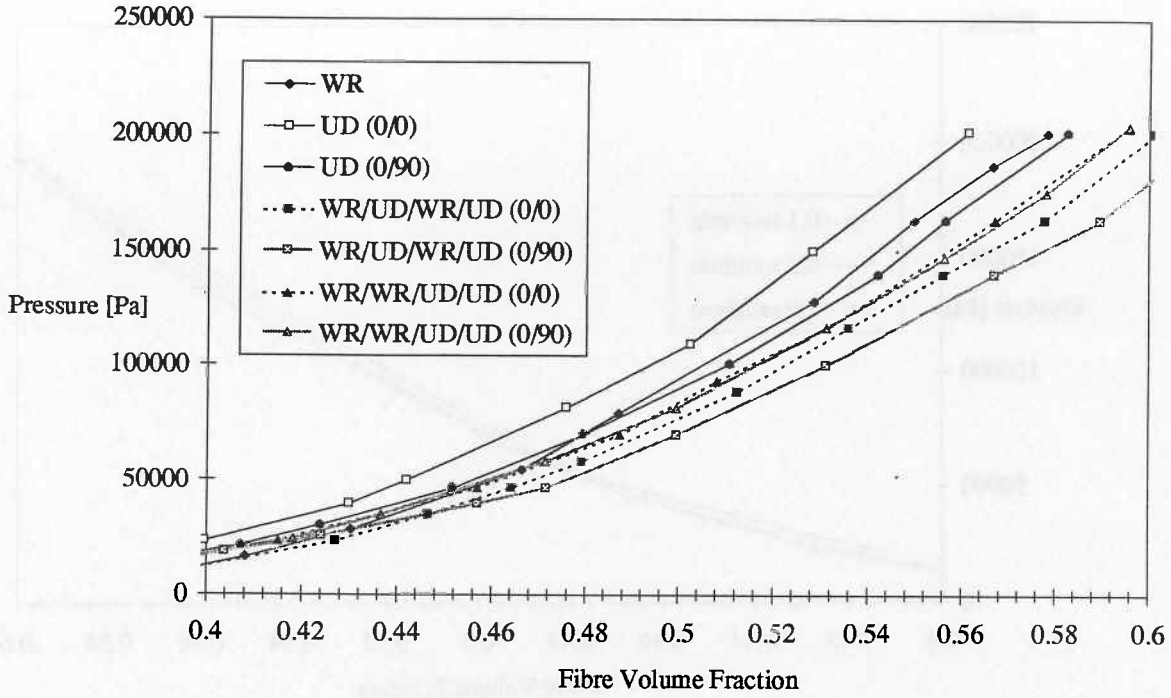

Figure 5 Compaction pressure versus fibre volume fraction (UD = quasi-unidirectional fabric, WR = woven roving, (0/90) means that the first layer of the UD material is aligned with the longer side of the platens while the second layer is at 90° to that direction)

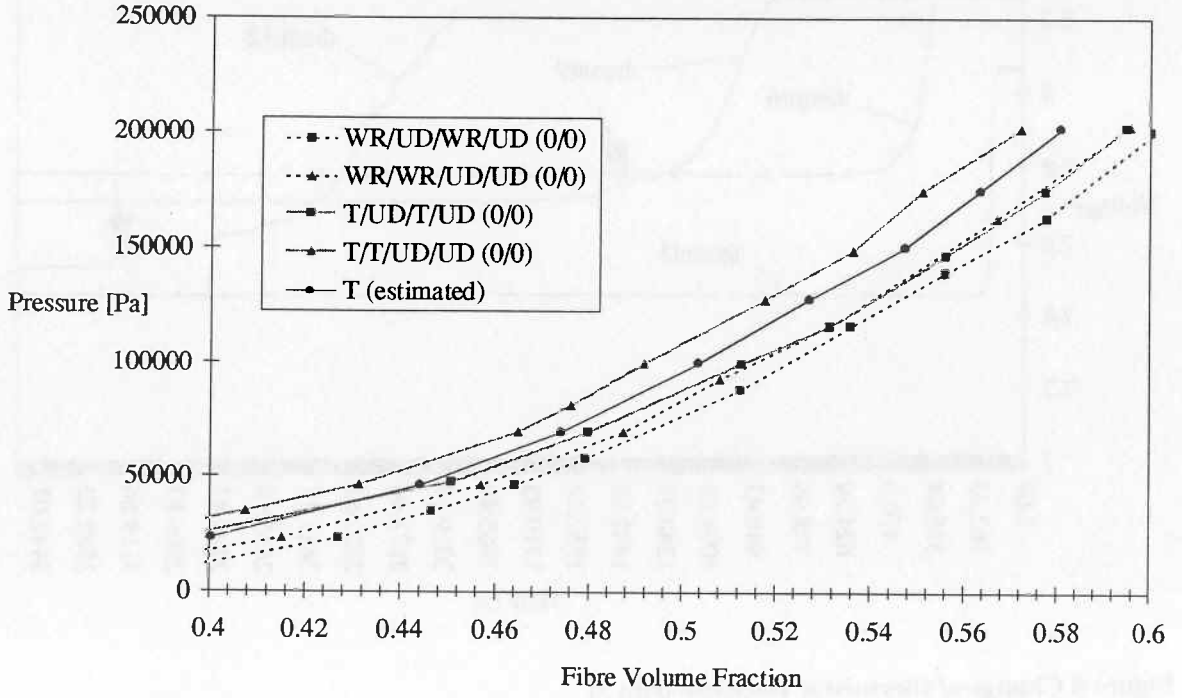

Figure 6 Compaction pressure versus fibre volume fraction (UD = quasi-unidirectional fabric, T = twill fabric, WR = woven roving, all layers of the UD material are aligned with the longer side of the platens)

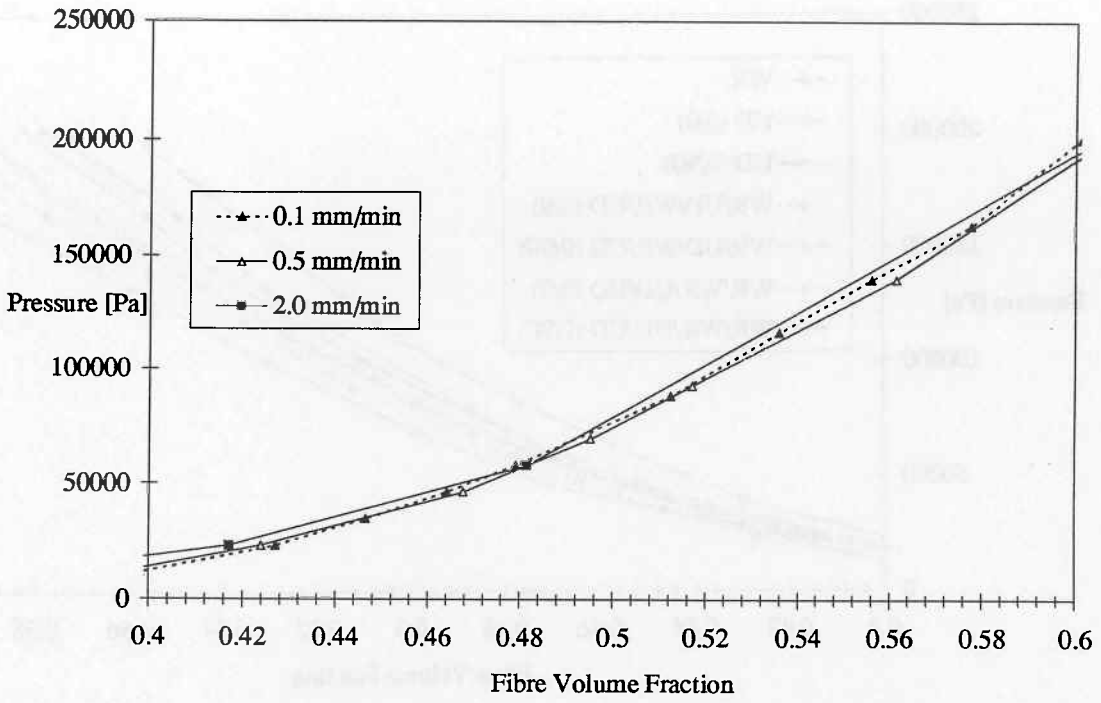

Figure 7 Compaction pressure for different closing speeds (WR/UD/WR/UD (0/0))

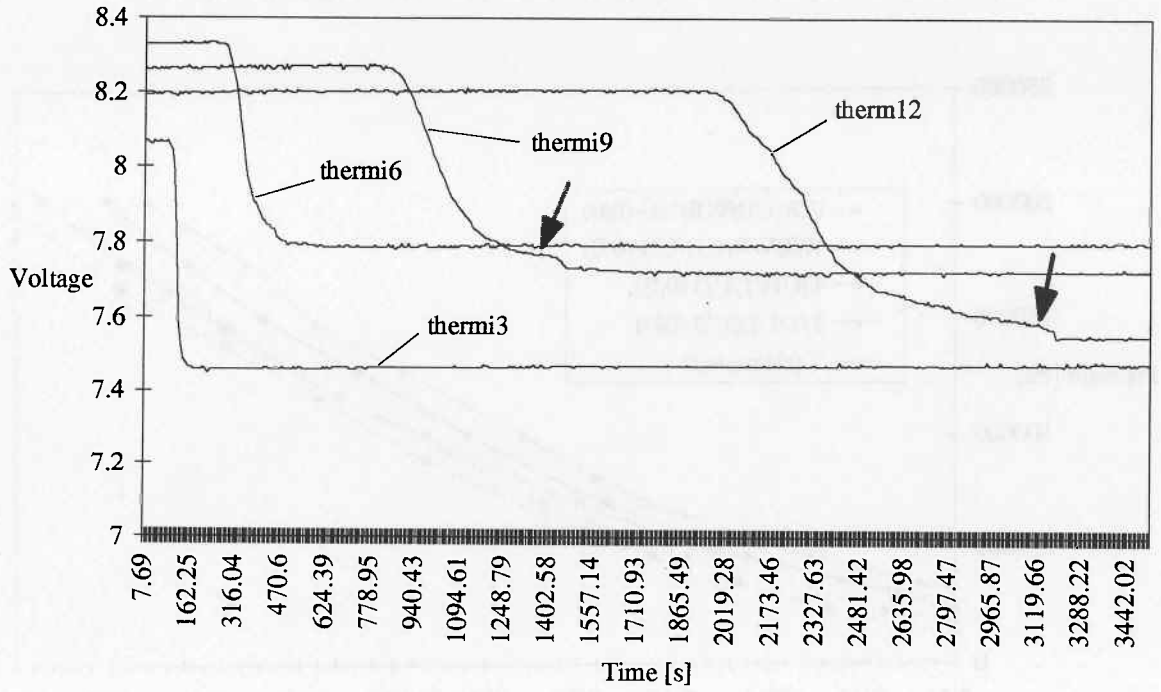

Figure 8 Change of thermistor response (run 5)

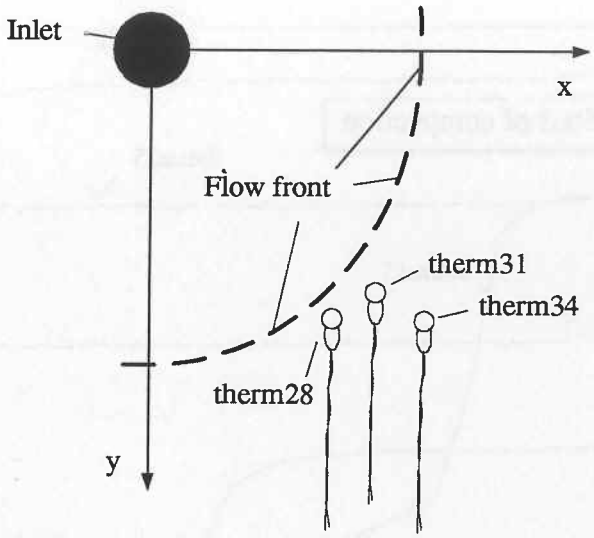

Figure 9 Measurement of flow front orientation (run7)

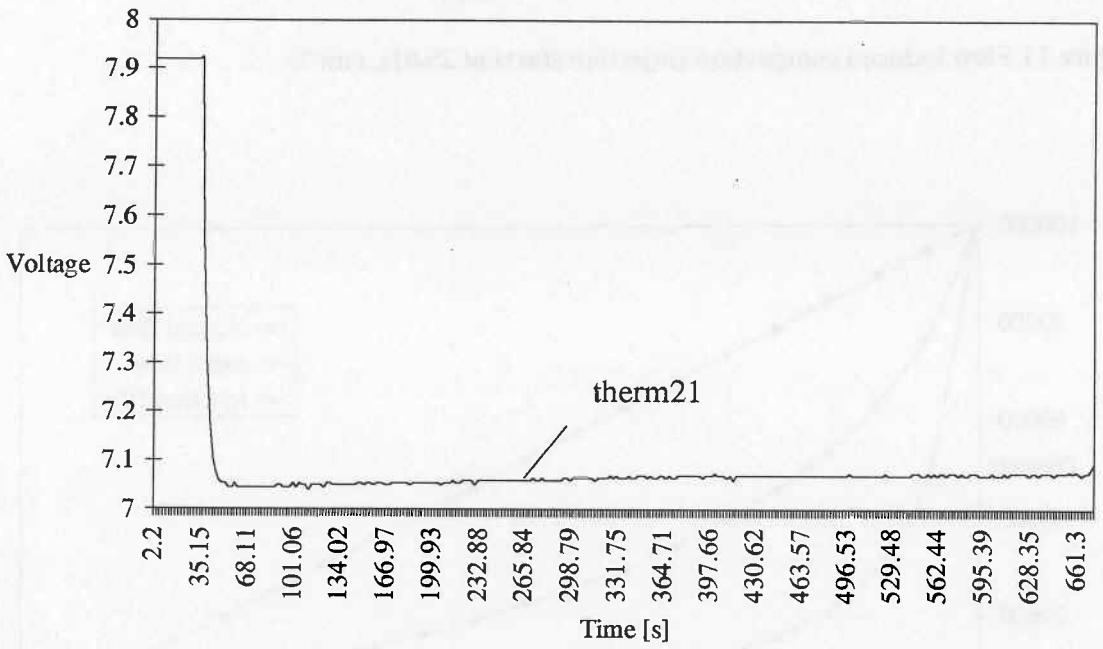

Figure 10 Velocity dependence of thermistor reading (run 3)

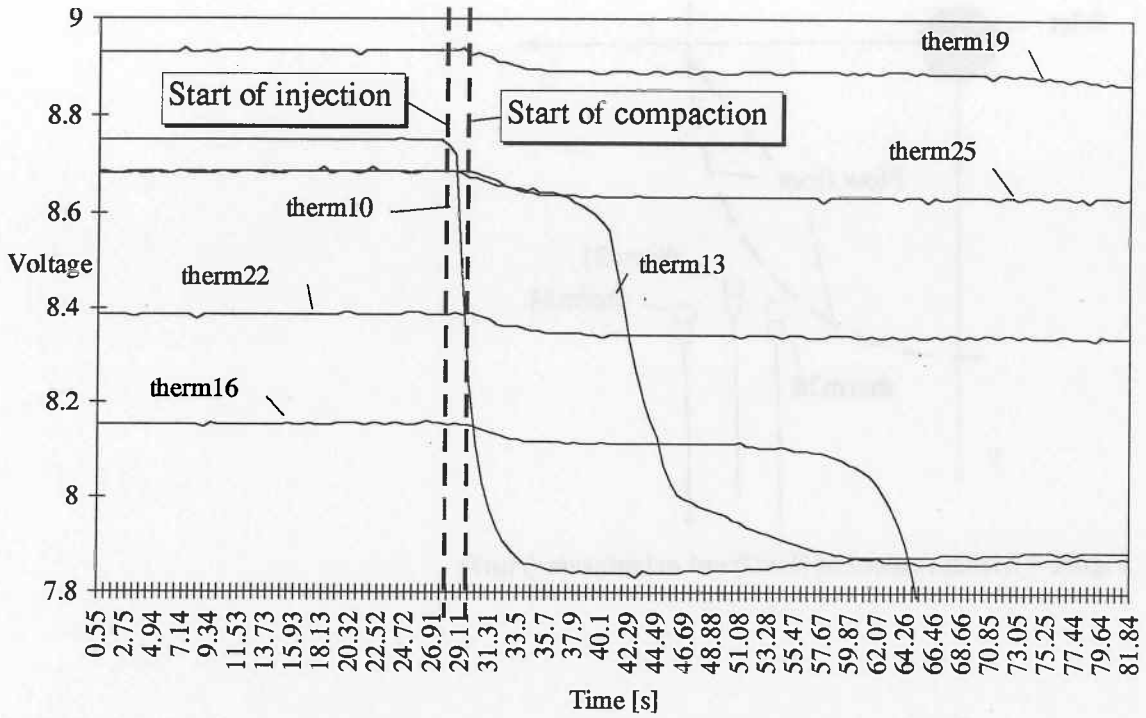

Figure 11 Flow induced compaction (injection starts at 28.01s, run 7)

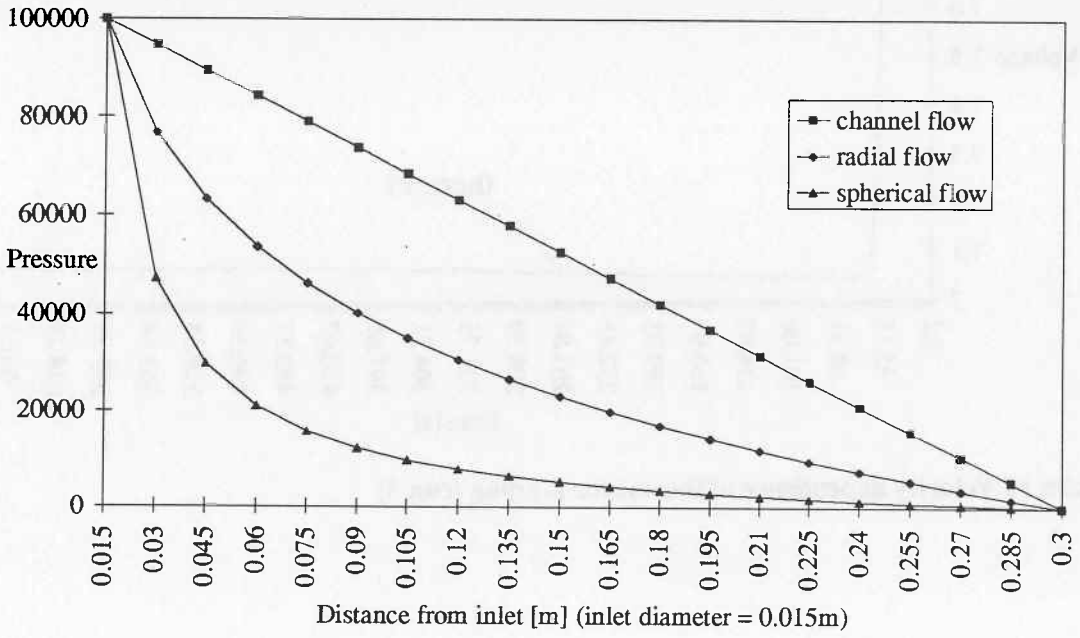

Figure 12 Pressure distribution for a given flow front length

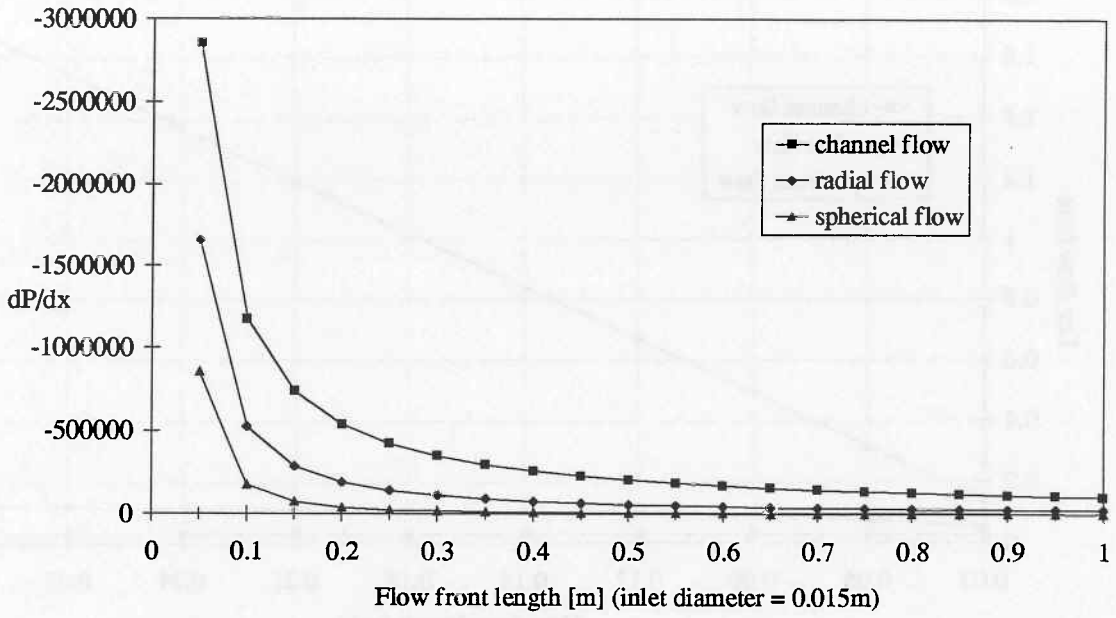

Figure 13 Pressure gradient at flow front

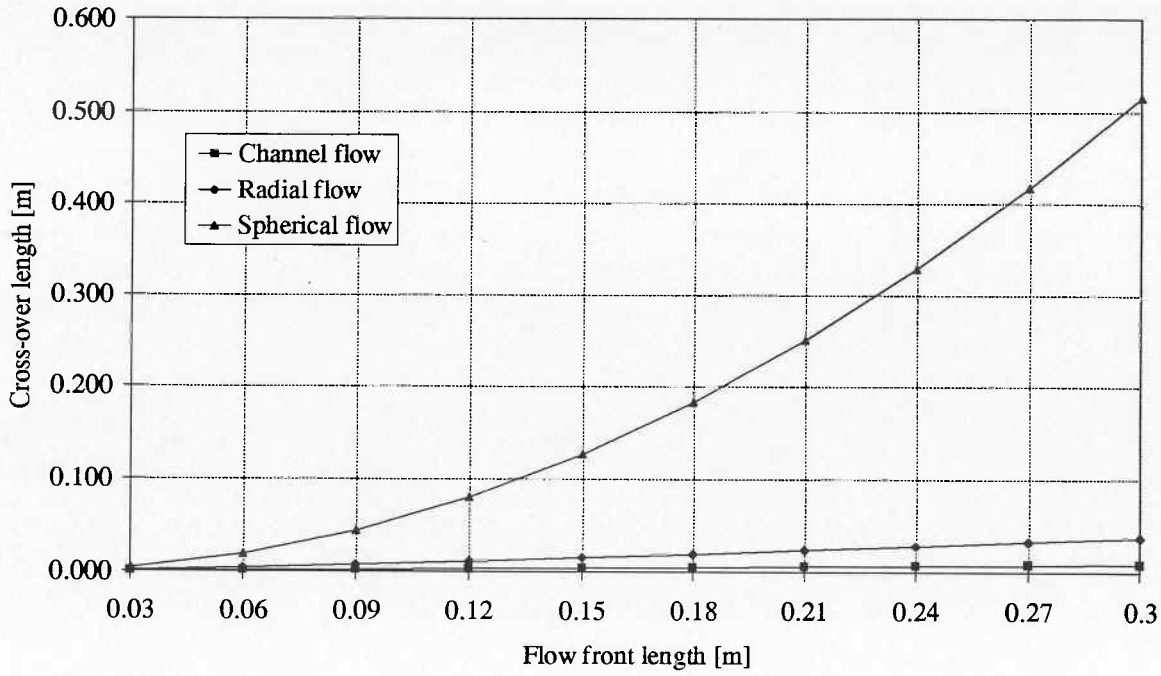

Figure 14 Cross-over length

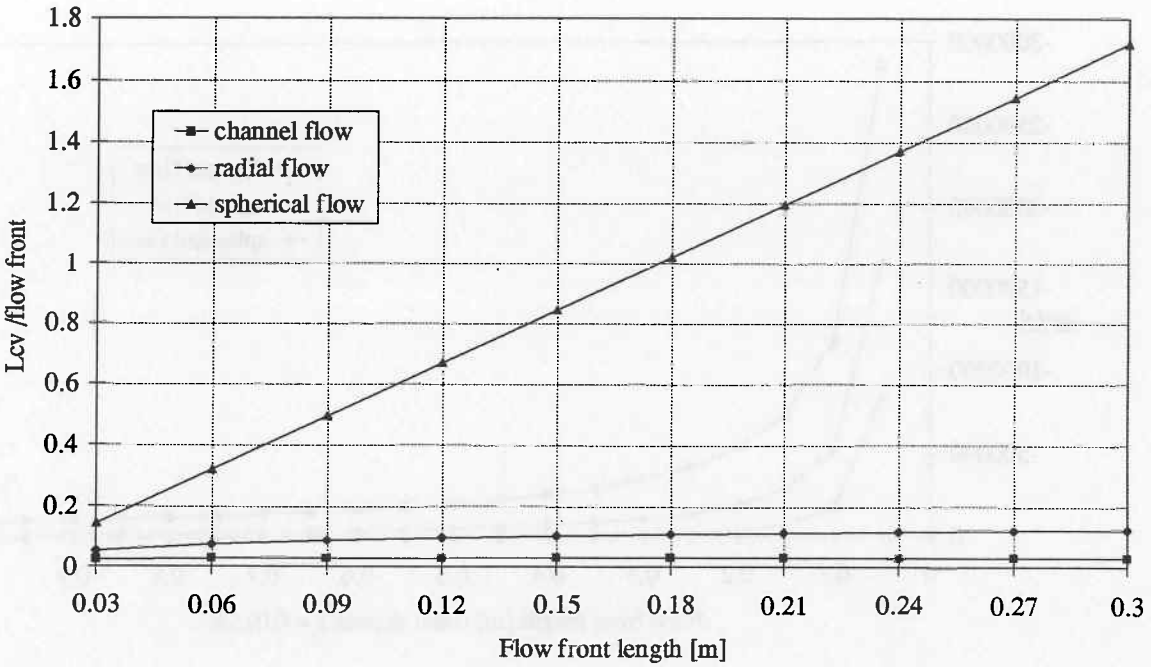

Figure 15 Ratio of cross-over length to flow front position